SUPPLEMENTAL MATERIAL

Supplemental Methods

Microcontact Printing of Parallel Fibronectin Lines

Parallel fibronectin protein lines for culture of cell strands were prepared similar to previously described methods[1] and as depicted in Figure I in the online-only Data Supplement. Briefly, silicon wafers were coated with a 10 µm-thick layer of photoresist (SU-8 10, Microchem), exposed to UV light through a patterned photomask, and developed to produce a negative of the desired pattern. Polydimethylsiloxane (PDMS) was poured onto the patterned wafer, cured overnight at 80°C, and removed to yield PDMS stamps of the desired micropattern (10 mm-long, 150 µm-wide parallel lines, spaced 300 µm apart connected on only one end). This micropattern design enabled simultaneous recording of up to three cell strands in the same field of view (1.95 mm at 10x magnification) during subsequent optical mapping studies (see Movie I in the online-only Data Supplement). For microcontact printing of fibronectin, the stamps were sonicated in 70% ethanol for one hour, washed in PBS, dried, and coated with 30 µg/mL fibronectin (Sigma) for one hour at room temperature. The stamp was briefly dried using a nitrogen air gun, and then gently pressed onto a 22 mm-diameter PDMS-coated coverslip to transfer the fibronectin protein pattern. After one hour, the stamp was removed and unstamped areas were coated with 0.2% w/v Pluronic F-127 (Molecular Probes) for 30 minutes to prevent cell growth between the patterned lines.

Derivation of Genetically Engineered Donor Cell Lines

The two donor excitable HEK293 cell lines (Excitable Slow or “ExS” and Excitable Fast or “ExF”) were derived as previously described.[2] Briefly, the ExS monoclonal cell line was generated by the subsequent transfection of Kir2.1-IRES-mCherry and $Na_v1.5$-IRES-GFP plasmids in

HEK293 cells followed by monoclonal selection of a stable cell line. The resulting ExS cells show poor intercellular coupling due to their low endogenous expression of gap junctions.[2, 3] The monoclonal ExF cell line was generated by the additional transfection of the ExS line with a Cx43-IRES-mOrange plasmid followed by monoclonal selection. Thus, the ExF cells (that we formerly referred to as Ex293)[2] have the same action potential properties as ExS cells (due to common monoclonal expression of $Na_v1.5$ and Kir2.1) and, in addition, show strong intercellular coupling due to the overexpression of Cx43 (Figure IIID in the online-only Data Supplement). The ExF and ExS donor cell lines were cultured in low glucose DMEM (Gibco #11885) supplemented with 10% FBS (Hyclone), a 1% penicillin-streptomycin solution (Gibco), and 1 mg/mL Puromycin (to maintain stable plasmid overexpression). The donor ExF and ExS cells were trypsinized, resuspended in growth media and seeded onto micropatterned strands as described below.

Neonatal Rat Ventricular Myocyte (NRVM) Isolation

All studies conformed to the Guide for the Care and Use of Laboratory Animals published by the United States National Institutes of Health (Publication No. 85-23, revised 1996) and all animals were treated in accordance with protocols approved by the Duke University Institutional Animal Care and Use Committee (IACUC). NRVMs were isolated from the ventricles of 2-day-old neonatal Sprague-Dawley rats (Charles River Laboratories) by enzymatic digestion with trypsin and collagenase, as previously described.[4] A highly-enriched cardiomyocyte suspension was generated following two one-hour differential preplating steps used to remove faster-adhering non-cardiomyocytes (eg, cardiac fibroblasts). Freshly isolated cardiomyocytes were suspended in low glucose DMEM (Gibco #11885) supplemented with 5% FBS (Hyclone) and 100 µmol/L Bromodeoxyuridine (BrdU, Sigma) to inhibit fibroblast proliferation and then seeded onto micropatterned strands as described below.

Cell Seeding of Micropatterned Host, Donor, and Host-Donor Strands

Prior to cell seeding, a PDMS stencil in the shape of a square frame with a thin (~ 300 μm-wide) dividing wall was sterilized in 70% ethanol, thoroughly washed and dried, and adhered either parallel to (host-only and donor-only strands) or perpendicular to (for host-donor strands) the stamped fibronectin lines (Figure 1). The use of this thin PDMS frame enabled separate and simultaneous seeding of host NRVMs ($2x10^3$ cells per mm^2) on one half of the fibronectin lines and donor engineered ExF or ExS cells ($0.3x10^3$ cells per mm^2) on the other half of the lines. While NRVMs were seeded in media containing 100 μmol/L BrdU, the ExS and ExF cells were not exposed to BrdU. Sixteen hours after cell seeding, the cultures were washed three times in culture media consisting of low glucose DMEM (Gibco #11885) supplemented with 5% FBS (Hyclone) and a 0.5% penicillin-streptomycin solution (Gibco) to remove unattached cells. While no paracrine effects of donor HEK293 cells on cardiomyocytes were previously observed,[5] the PDMS frames were designed such that coverslips with homocelluar (host-only or donor-only) and heterocellular (host-donor) strands had similar ratios of NRVMs and HEK293 cells and maintained under similar culture conditions.

After cell attachment and washing, the PDMS frame was removed and, in the case of the host-donor strands, the subsequent proliferation and migration of donor ExF or ExS cells across the remaining acellular gap formed a seamless interface with the host NRVMs (Figure IIIA and IIIB in the online-only Data Supplement). The stamped micropattern allowed the NRVM ends of strands to connect into a large common area which enabled synchronization of their spontaneous activity and supported cell spreading to confluence.[6] Homocellular NRVM, ExF, and ExS strands were utilized for analysis of APD and CV restitution profiles (Figure II in the online-only Data Supplement) while the heterocellular NRVM-ExF and NRVM-ExS strands were used for analysis of APD dispersion and vulnerability to block during a premature stimulus. Prior to optical mapping (day 4-5 after cell seeding), the strands were electrically isolated from one another by cutting across the junctions between the strands and the common area using a

scalpel and dissecting microscope. This allowed mapping in each strand to be treated as an independent experiment.

Through the use of donor engineered excitable cells that have a short APD and predominantly rely on I_{K1} for repolarization, we created a platform whereby $BaCl_2$ inhibition of I_{K1} selectively altered APD in donor cells thus enabling controlled manipulation of APD dispersion across the host-donor cell interface. Specifically, the two doses of $BaCl_2$ (25 µmol/L and 50 µmol/L) were used to selectively prolong the APD of the donor cells without significantly altering the APD of host NRVMs or CV in any of the cells (Figure II and Table I in the online-only Data Supplement). Higher doses of $BaCl_2$ caused APD prolongation in NRVMs and CV reduction in all cells, likely by depolarizing membrane potential and reducing Na^+ current availability, as previously shown by others[7] and us.[2]

Microscopic Optical Mapping of Transmembrane Voltage in Micropatterned Strands

We utilized narrow micropatterned cell strands of 150 µm width (smaller than the monolayer resting space constant)[8] to generate a simple pseudo-1-dimensional propagation pattern that could be readily assessed by optical mapping. Action potential propagation in the patterned cell strands was optically mapped on culture days 5 and 6 using an array of 504 hexagonally arranged optical fibers (connected to a photodiode array, PDA) positioned against an image intensifier (XR5, Photonis) connected to the side port of an inverted microscope (Nikon TE-2000U Eclipse) as previously described.[9] At 10x magnification, this yielded a single channel resolution of 75 µm and total field of view of 1.95 mm. Cell cultures were incubated with the voltage-sensitive dye, ANNINE-6plus (5 µg/mL, Sensitive Dyes GbR)[10] for 5 minutes at room temperature and then transferred to a temperature-controlled chamber perfused with Tyrode's solution. Illumination was provided by a mercury light source (130 W, Intensilight, Nikon) controlled by a fast electronic shutter (Optiquip). The ANNINE-6plus dye was excited through a 480±50 nm excitation filter (Chroma) and emitted fluorescence collected through a 565 nm long-

pass emission filter (Chroma) and objective lens before being amplified by the image intensifier and transmitted onto the PDA. The optical recordings were converted to voltage signals, amplified, and sampled at 2.4 kHz. Blebbistatin (5 μmol/L, Sigma) was added to the Tyrode's solution to prevent motion artifacts[11] and enable accurate recording of AP repolarization. At the end of each experiment, AP shape and CV were compared to those measured at the beginning in each strand to ensure cell health and consistency in data. Data was discarded if it was found that this consistency was not maintained during the experimental recording.

The use of fluorescent donor cells allowed us to unambiguously identify the host-donor cell interface within each strand, while simultaneous excitation and mapping of multiple strands (see Movie I in the online-only Data Supplement) was performed to increase experimental throughput. The monolayer preparations also precluded depth-averaging artifacts (that may occur during mapping of thicker 3-D tissues)[12, 13] thereby enabling accurate recording and quantification of the resulting AP gradients. Typically, micropatterned cardiomyocyte strands have previously been used to track the activation front of a propagating AP at magnifications from 20-100x and for short time periods (<300 ms).[14-20] Importantly, the ability to map activation and repolarization wavefronts during multiple S1-S2 intervals in our studies required an increase in the total recording time to several tens of seconds which was accomplished by combining the use of an image intensifier, a high SNR voltage sensitive dye (ANNINE-6plus),[10] and mapping at lower (10x) magnification as described above.

Spatial Co-registration of Host-Donor Strands and Photodiode Array

To spatially co-register the optical mapping signals with their site of origin on the cell strand, brightfield and fluorescence (to identify donor cells) images were taken by a CCD camera (SensiCam QE, Cooke) at the end of each experiment (Figure 2A). Based on a previously described method for overlay of and registration between optical fiber positions and pixels in the CCD image,[1] the acquired optical mapping signals were precisely assigned the location on the

host-donor strand. The host-donor interface position was set to “0 mm” on the *x*-axes of all plots. Negative *x* values denoted positions to the left of the interface (ie, the donor cell half of the strand) while positive *x* values denoted positions to the right of the interface (ie, the host cell half of the strand).

Pacing Protocols in Micropatterned Strands

During microscopic optical mapping, two bipolar XYZ-micropositioned platinum line electrodes were positioned at two ends of host-donor strands and used to initiate electrical propagation at a basic rate of 2 Hz (at 1.2x threshold) ~4-5 mm away from the heterocellular interface. Pacing from either the host NRVM or the donor engineered HEK293 end of each strand allowed us to assess influence of propagation direction on the spatial profile of activation, repolarization, and APD across the host-donor interface. The S1-S2 pacing protocol was performed by pacing the strands at a basic rate of 2 Hz for 30 pulses (S1) followed by a premature stimulus (S2) of the same amplitude. The S1-S2 time interval was decreased until the S2 pulse failed to initiate an action potential. This pacing protocol was used both to construct S1-S2 restitution curves of action potential duration and conduction velocity for each cell type (in host-only or donor-only strands) as well as to quantify the vulnerable window (VW) for S2 conduction block in host-donor strands.

Data Analysis

For the recorded signal in each optical channel, activation was considered successful when the first derivative of the transmembrane potential (maximum upstroke velocity, dV_m/dt_{max}) exceeded an empirically defined threshold of activation. The site of conduction failure (block) was identified as the most proximal recording site with a subthreshold dV_m/dt_{max} value and manually confirmed with single-pixel (75 μm) resolution by identifying an abrupt change in the uniformity of the isochrone activation map.[9] For optical channels exhibiting an action potential, activation

times (AT), defined as the instance of dV_m/dt_{max}, action potential duration at 80% repolarization (APD), and repolarization time at 80% repolarization (RT), were determined using custom MATLAB software, as previously described.[9]

Activation and repolarization times were averaged among recording sites across the width of each strand and reported every 0.065 mm along the length of the strand. Plots of AT versus distance (x) along the strand were fit linearly (in NRVM-only, ExF-only, ExS-only, or NRVM-ExF strands) or bilinearly (in NRVM-ExS strands) and used to calculate host and donor average conduction velocities (CVs). Spatial profiles of APD or RT across the heterocellular interface as a function of x were fit with a sigmoidal Boltzmann function of the form $y = y_0 + \frac{y_\infty - y_0}{1+\exp\left(\frac{-(x-x_{1/2})}{b}\right)}$ and used to calculate the maximum slope (∇APD_{max} or ∇RT_{max}, in ms/mm) of the fit ($\frac{y_\infty - y_0}{4b}$) similar to that done by Restivo et al.[21] The heights (Δy) of APD and RT profiles (in ms) were defined as the difference between 10% and 90% of (y_∞-y_0), while the widths (Δx) of APD and RT profiles (in mm) were reported as the distance on the x axis corresponding to Δy (see Figure IVC in the online-only Data Supplement). The magnitudes of the spatial gradients of activation and repolarization measured at 10x magnification were consistent with those measured during optical mapping at higher magnifications (20 and 40x) and/or without the use of the image intensifier.

The vulnerable time window for conduction block (VW) was defined as the time difference between the maximum S1-S2 interval that resulted in S2 conduction block across the host-donor interface and the maximum S1-S2 interval that resulted in S2 block near the donor cell pacing site (as shown in Figure VI in the online-only Data Supplement). The VW for S2 block in each heterocellular strand was then plotted against the corresponding APD and RT spatial profile parameters quantified for the prior S1 stimuli recorded in that strand to determine if any correlation existed (as determined by linear regression) between VW and the height, spatial width, or maximum gradient of RT or APD across the host-donor interface.

Immunostaining and Cell Imaging

Cultures were fixed and permeabilized in a solution of 2% paraformaldehyde (PFA, diluted in PBS) and 1% Triton-X (Sigma, Triton-X100 diluted in PBS) for 4 minutes at room temperature, placed into a solution of 2% PFA for an additional 10 minutes at RT, and then blocked in a solution of 1% bovine serum albumin (BSA, Sigma) and chicken serum (Gibco) in a 5:1 ratio for one hour at room temperature. Primary antibodies, including anti-sarcomeric α-actinin (Sigma, EA-53 mouse monoclonal) and anti-connexin-43 (Zymed, rabbit polyclonal), were applied overnight at 4^{o}C. Secondary antibodies, including Alexa Fluor 488 (chicken anti-rabbit), Alexa Fluor 594 (chicken anti-mouse), or FITC conjugated anti-green fluorescent protein (α-GFP) were applied for 1 hour at room temperature. Nuclei were counterstained with 4',6-diamidino-2-phenylindole (DAPI, Sigma). Brightfield phase-contrast and fluorescence images of live or immunostained cultures were acquired using a CCD camera (SensiCam QE, Cooke) attached to an inverted microscope (Nikon TE2000). A 10x Plan Apo (0.45 numerical aperture, Nikon) objective was used for both imaging and mapping.

Statistical Analysis

We tested the normality of our data using the D'Agostino-Pearson omnibus K2 test (when sample size was ≥8) or the Kolmogorov-Smirnov one-sample goodness-of-fit test (when sample size was <8). Data presented as mean±SEM and were evaluated for statistical significance by linear regression, two-tailed paired or unpaired t-tests, or one-way ANOVAs (regular ANOVA to analyze data obtained from different strands or repeated measures ANOVA to analyze data obtained from the same strands) with post hoc Tukey's test for multiple comparisons using GraphPad Prism (GraphPad Software, Inc.). Differences were considered statistically significant at $P<0.05$ and different levels of significance were defined as $*P<0.05$, $**P<0.01$, and $***P<0.001$.

Supplemental Results

Rate Dependence of APD and CV in Homocellular Host and Donor Strands

S1-S2 action potential duration (APD) and conduction velocity (CV) restitution curves were measured in micropatterned homocellular strands made of host NRVMs, donor ExS or donor ExF cells in the presence of 0 (control), 25, or 50 μmol/L $BaCl_2$ (Figure II and Table I in the online-only Data Supplement). Under control conditions, the APD of the ExF and ExS cells were similar (eg, 31.9±0.7 and 34.6±1.1 ms, respectively, at S1-S2=500 ms) and significantly shorter than that of the NRVMs (eg, 153.2±2.3 ms at S1-S2=500 ms). CVs in the NRVMs and ExF cells were similar at long S1-S2 intervals (eg, 22.3±0.3 and 22.1±0.4 cm/s, respectively, at S1-S2=500 ms) but diverged during shorter intervals when the NRVM CV sharply decreased (bottom, Figure IIA in the online-only Data Supplement). The fast CV in ExF strands compared to ExS strands (3.1±0.1 cm/s at S1-S2=500 ms) resulted from the additional overexpression of Cx43 in the ExF cells. Weak intercellular coupling between the ExS cells was mediated by endogenous HEK293 gap junctions other than Cx43.[2] Application of 25 μmol/L (Figure IIB in the online-only Data Supplement) or 50 μmol/L (Figure IIC in the online-only Data Supplement) $BaCl_2$ significantly prolonged the APD of ExF and ExS cells to comparable levels (69.8±1.7 and 68.5±1.4 ms at 25 μmol/L $BaCl_2$ and 139.1±4.1 and 137.6±2.9 ms at 50 μmol/L $BaCl_2$ for the ExF and ExS cells, respectively), but did not alter the APD of NRVMs (161.5±4.6 and 164.2±5.6 ms at 25 μmol/L and 50 μmol/L $BaCl_2$, respectively). Similarly, CV restitution curves in NRVM strands were not altered by the $BaCl_2$ application, while in both ExF and ExS strands, the greater conduction slowing during premature excitation induced by $BaCl_2$ eventually yielded conduction failure at a longer S1-S2 interval (Figure IIB and IIC, bottom panels, and Table I in the online-only Data Supplement). All conduction blocks eventually occurred at the vicinity of the pacing site. Overall, applying 25 and 50 μmol/L $BaCl_2$ increased APDs and selectively decreased CVs at short S1-S2 intervals in the engineered excitable cells while having no effect on the restitution curves of NRVMs.

Supplemental Tables

Online Table I. Parameters of S1-S2 restitution in homocellular strands

Homocellular Strand	+/- $BaCl_2$	S1-S2=500 ms APD (ms)	S1-S2=500 ms CV (cm/s)	minimum S1-S2 (ms)	min. S1-S2 APD (ms)	min. S1-S2 CV (cm/s)
NRVM	0 μM $BaCl_2$	153.2±2.3*	22.3±0.3	151.7±3.2*	100.3±1.5*	14.2±0.3*
ExF	0 μM $BaCl_2$	31.9±0.7	22.1±0.4	43.6±1.0*	27.2±0.7	19.1±0.6*
ExS	0 μM $BaCl_2$	34.6±1.1	3.06±0.06*	56.9±1.9*	25.9±0.5	1.81±0.03*
NRVM	25 μM $BaCl_2$	161.5±4.6*	21.4±0.6	156.7±1.7*	107.6±5.7*	14.2±0.6
ExF	25 μM $BaCl_2$	69.8±1.7	21.4±0.5	86.7±0.7	52.4±1.6	14.6±0.3
ExS	25 μM $BaCl_2$	68.5±1.4	3.18±0.10*	85.8±0.6	47.2±1.6	2.03±0.2*
NRVM	50 μM $BaCl_2$	164.2±5.6*	21.9±0.7	157.9±5.9*	117.2±6.3	13.9±0.4*
ExF	50 μM $BaCl_2$	139.1±4.1	21.0±0.4	146.3±1.8	101.6±2.3	11.2±0.2*
ExS	50 μM $BaCl_2$	137.6±2.9	3.04±0.04*	144.1±3.4	92.6±2.0	2.02±0.02*

Measured after 30 prepulses (S1-S1=500 ms), mean±SEM, n=5-13 per group. ANOVA with post hoc Tukey's test for mulitiple comparisons, *P<0.05 compared to other cell types within same $BaCl_2$ treatment group.

Online Table II. Linear regression results of RT profile parameters vs. vulnerable window (VW)

	0 μM $BaCl_2$		25 μM $BaCl_2$		50 μM $BaCl_2$		All Doses Combined	
	ExF-NRVM	ExS-NRVM	ExF-NRVM	ExS-NRVM	ExF-NRVM	ExS-NRVM	ExF-NRVM	ExS-NRVM
Δy RT vs. VW r^2=	---	---	---	---	0.71	0.38	0.87	0.84
Δx RT vs. VW r^2=	0.25	0.53	0.29	0.44	---	---	0.56	0.69
∇RT_{max} vs. VW r^2=	0.84	0.78	0.77	0.79	0.81	0.91	0.91	0.90
n=	19	18	21	19	16	16	56	53

"---", linear regression slope not significantly different from zero.

Supplemental Figures and Figure Legends

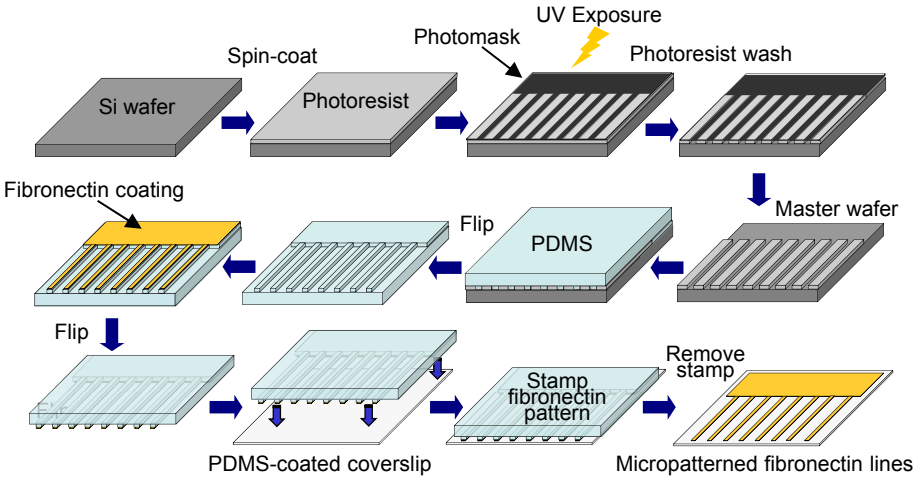

Online Figure I. Micropatterning of fibronectin lines for cell strand cultures. Polydimethylsiloxane (PDMS) stamps, fabricated using standard soft lithography techniques, were used to print 150 μm-wide fibronectin lines spaced 300 μm-apart onto PDMS-coated coverslips prior to cell seeding.

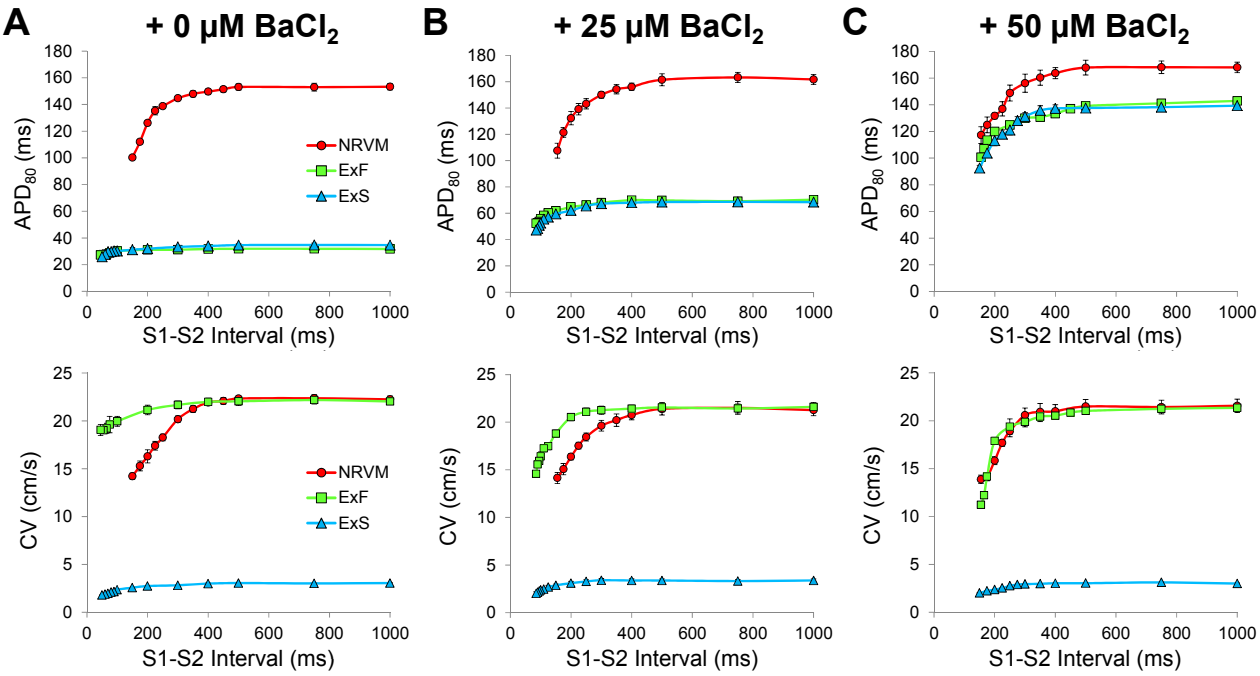

Online Figure II. APD and CV restitution curves in NRVM, ExF, and ExS homocellular strands. **A-C**, APD (**top**) and CV (**bottom**) S1-S2 restitution curves in the presence of 0, 25 or 50 μmol/L $BaCl_2$. Thirty S1 stimuli at basic cycle length of 500 ms were followed by a premature S2 stimulus (n=5-13 per group). All data displayed as mean±SEM. See Table I in online-only Data Supplement for numerical values and statistics.

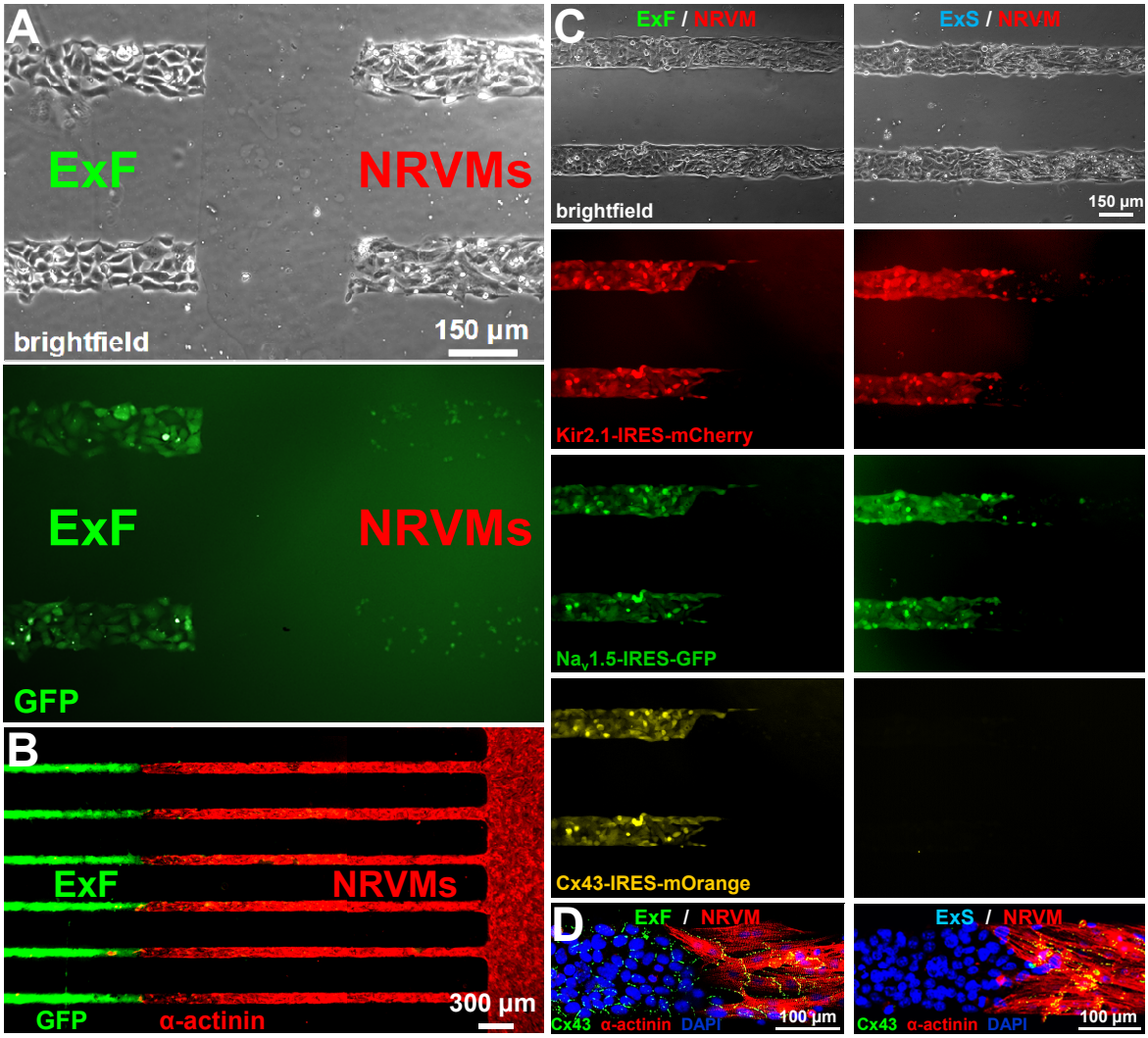

Online Figure III. Live fluorescence and immunostained images of heterocellular strands. **A,** Brightfield (**top**) and flourescence (**bottom**) images after cell attachment and upon removal of perpendicular PDMS frame show acellular gap between GFP$^+$ ExF cells and NRVMs. **B,** After 2-3 days, proliferating ExF cells populate the acellular gap and form a seamless heterocellular interface with NRVMs (composite image). **C,** Brightfield and fluorescence imaging was then used to identify the location of the engineered cells (ExF or ExS) within the heterocellular strands in relation to non-fluorescent NRVMs to localize interface prior to optical mapping. ExS cells lack expression of Cx43-IRES-mOrange (**bottom right**). **D,** Immunostained images of interface between NRVMs (expressing sarcomeric alpha-actinin, **red**) and either well-coupled, Cx43 expressing (**green**) ExF cells (**left**) or poorly-coupled ExS cells that lack Cx43 gap junctions (**right**).

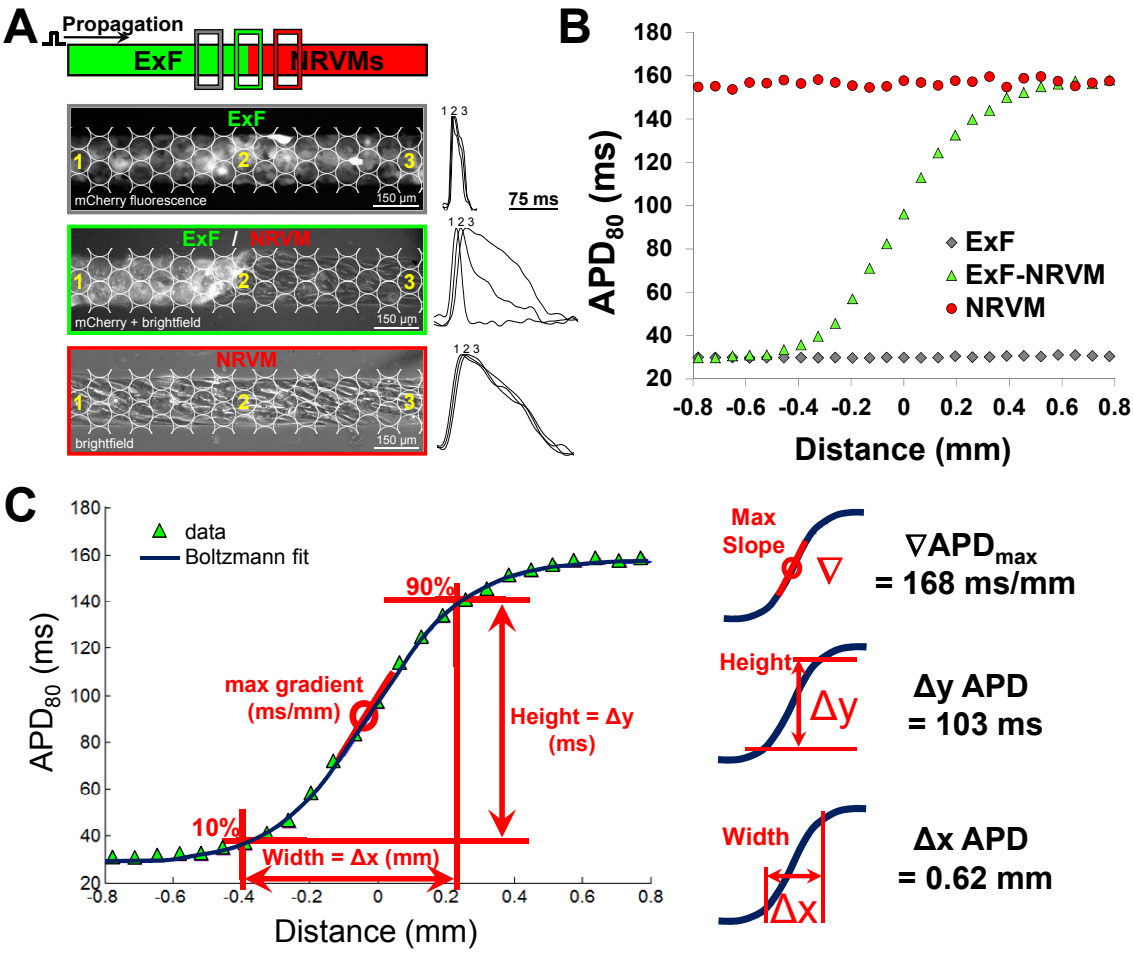

Online Figure IV. Quantification of the shape of spatial APD profile across a heterocellular interface. **A-B**, Example of optical mapping of propagating APs (AP traces shown **on right**) at three locations within a heterocellular ExF-NRVM strand (**green frame**, ExF only region; **gray frame**, ExF-NRVM interface region; **red frame**, NRVM only region). Small circles denote optical recording sites during 10x micromapping. **B,** Spatial profile of action potential duration at 80% repolarization (APD) corresponding to the 3 regions shown in **A**. For the green trace, position x=0 mm corresponds to the ExF-NRVM interface. **C**, A boltzmann sigmoidal fit of the APD profile was used to determine the height (Δy APD), width (Δx APD), and maximum slope (gradient, ∇APD_{max}) of the APD profile. The same fit procedure was applied to the spatial profile of repolarization time (RT) to derive Δy RT, Δx RT, and ∇RT_{max}. Data shown is representative sample from n=152 host-donor strands.

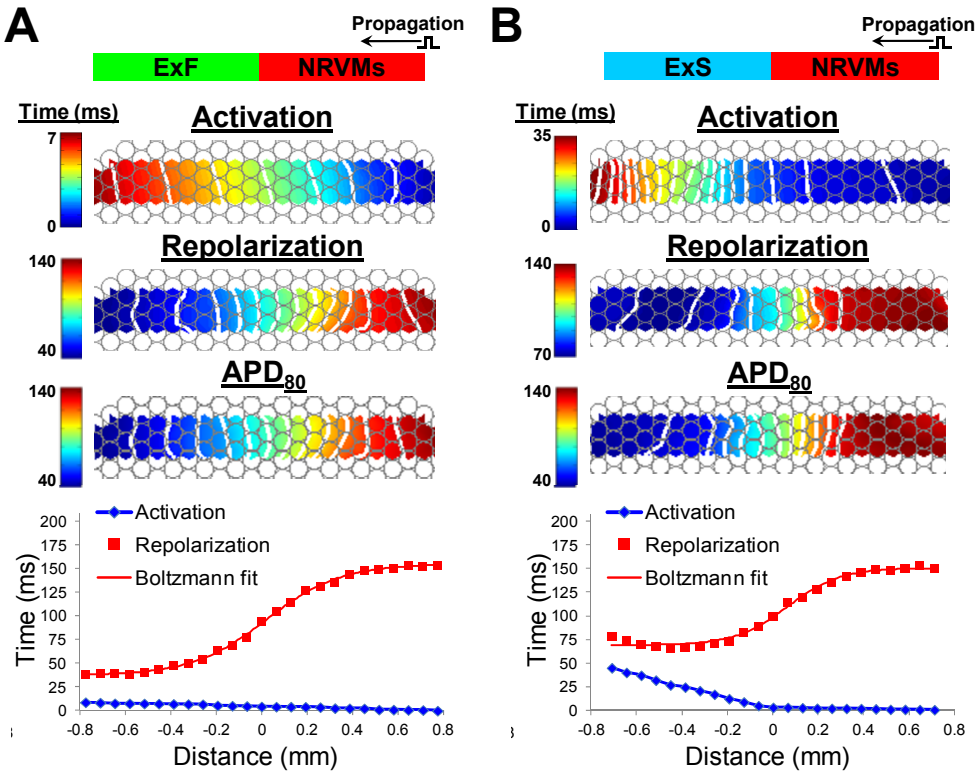

Online Figure V. Action potential propagation across host-donor interface initiated at the host end of the strand. **A-B**, Representative isochrone maps of activation (1 ms (**A**) or 2 ms (**B**) spacing), repolarization (10 ms spacing), and APD (10 ms spacing), as well as corresponding spatial profiles of activation (**blue**) and repolarization (**red**) shown for an ExF-NRVM (**A**) or ExS-NRVM (**B**) strand paced from the host NRVM end. Position of host-donor interface is assigned the coordinate x=0 mm. Shown is the 30th propagated AP during 2 Hz pacing. When the AP is propagated in the opposite (donor-to-host) direction in the same strands (Figures 2C and 2D), we found significant reduction in Δy RT (from 106.9±2.5 to 88.9±3.2 ms), Δx RT (from 0.54±0.02 to 0.49±0.02 ms), and ∇RT_{max} (from 199.6±7.1 to 184.4±7.9 ms, n=22 for all) for ExS-NRVM, but not ExF-NRVM, strands. This could be attributed to slow AP propagation in the poorly-coupled ExS cells which effectively flattened the RT profile (**B**, **bottom**). Data shown is representative sample from n=44 host-donor strands. Examples of AP conduction initiated at either end of host-donor strands are shown in Movie II in the online-only Data Supplement. Differences in activation and repolarization profiles observed between host-to-donor and donor-to-host AP propagation in heterocellular strands could be potentially encountered within native heart tissue as the AP propagates into and then back out of a donor cell graft.

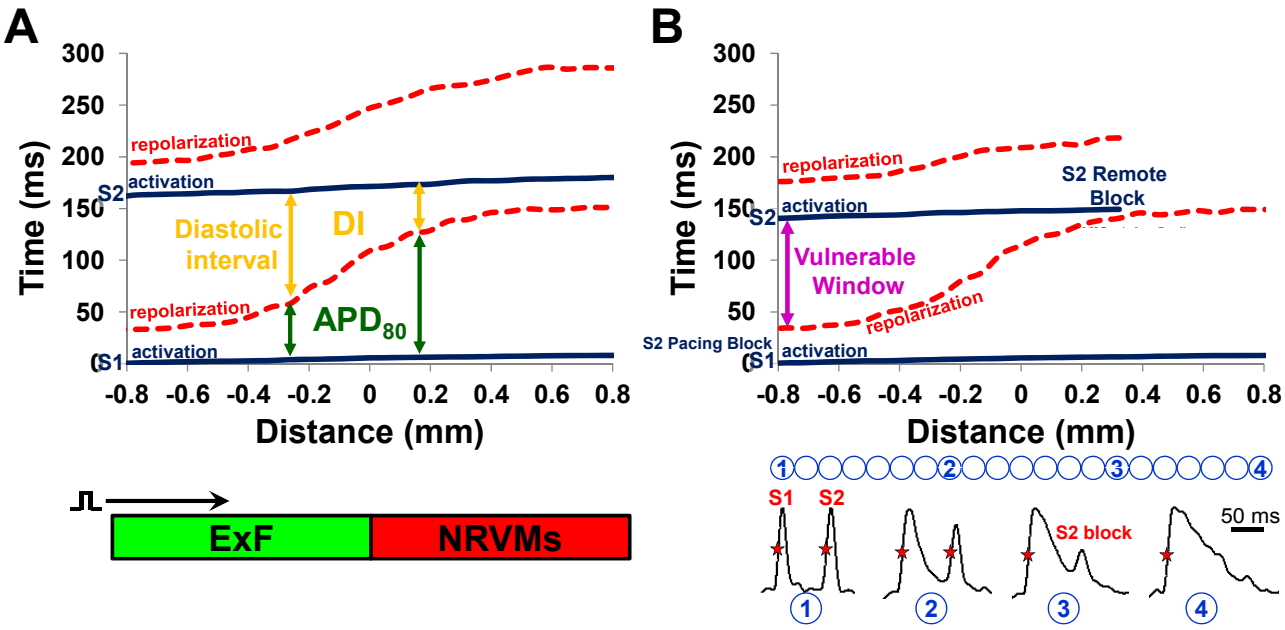

Online Figure VI. AP propagation during S1-S2 stimulation. **A,** Representative example of activation (**blue solid line**) and repolarization (**red dashed line**) time-space plots for a propagating S1 and S2 pulse (S1-S2=160 ms) in an ExF-NRVM strand. Position x=0 mm denotes the heterocellular interface. At any point along the strand, the S1 APD is represented by the difference between S1 repolarization and S1 activation times while diastolic interval (DI) is represented by the difference between S2 activation and S1 repolarization times. **B,** At a shorter S1-S2 interval (140 ms), a decrease in DI leads to decremental propagation of S2 (traces shown below) and conduction block at a site within the NRVM region (eg, site "3"). AP upstrokes (red stars) identify activation times of propagating AP. The difference between the maximum S1-S2 intervals yielding conduction block at the interface region vs. pacing site is defined as the vulnerable window (VW) for S2 block. Data shown is representative sample from n=109 host-donor strands.

Supplemental References

1. Klinger R, Bursac N. Cardiac cell therapy in vitro: Reproducible assays for comparing the efficacy of different donor cells. *IEEE Eng Med Biol Mag*. 2008;27:72-80.
2. Kirkton RD, Bursac N. Engineering biosynthetic excitable tissues from unexcitable cells for electrophysiological and cell therapy studies. *Nat Commun*. 2011;2:300.
3. McSpadden LC, Nguyen H, Bursac N. Size and ionic currents of unexcitable cells coupled to cardiomyocytes distinctly modulate cardiac action potential shape and pacemaking activity in micropatterned cell pairs. *Circ Arrhythm Electrophysiol*. 2012;5:821-830.
4. Badie N, Bursac N. Novel micropatterned cardiac cell cultures with realistic ventricular microstructure. *Biophys J*. 2009;96:3873-3885.
5. Pedrotty DM, Klinger RY, Kirkton RD, Bursac N. Cardiac fibroblast paracrine factors alter impulse conduction and ion channel expression of neonatal rat cardiomyocytes. *Cardiovasc Res*. 2009;83:688-697.
6. Rohr S, Scholly DM, Kleber AG. Patterned growth of neonatal rat heart cells in culture. Morphological and electrophysiological characterization. *Circ Res*. 1991;68:114-130.
7. Chan YC, Tse HF, Siu CW, Wang K, Li RA. Automaticity and conduction properties of bio-artificial pacemakers assessed in an in vitro monolayer model of neonatal rat ventricular myocytes. *Europace*. 2010;12:1178-1187.
8. Kleber AG, Rudy Y. Basic mechanisms of cardiac impulse propagation and associated arrhythmias. *Physiological reviews*. 2004;84:431-488.
9. Badie N, Scull JA, Klinger RY, Krol A, Bursac N. Conduction block in micropatterned cardiomyocyte cultures replicating the structure of ventricular cross-sections. *Cardiovasc Res*. 2012;93:263-271.
10. Fromherz P, Hubener G, Kuhn B, Hinner MJ. Annine-6plus, a voltage-sensitive dye with good solubility, strong membrane binding and high sensitivity. *Eur Biophys J*. 2008;37:509-514.
11. Fedorov VV, Lozinsky IT, Sosunov EA, Anyukhovsky EP, Rosen MR, Balke CW, Efimov IR. Application of blebbistatin as an excitation-contraction uncoupler for electrophysiologic study of rat and rabbit hearts. *Heart Rhythm*. 2007;4:619-626.
12. Baxter WT, Mironov SF, Zaitsev AV, Jalife J, Pertsov AM. Visualizing excitation waves inside cardiac muscle using transillumination. *Biophysical journal*. 2001;80:516-530.
13. Bray MA, Wikswo JP. Examination of optical depth effects on fluorescence imaging of cardiac propagation. *Biophysical journal*. 2003;85:4134-4145.
14. Gaudesius G, Miragoli M, Thomas SP, Rohr S. Coupling of cardiac electrical activity over extended distances by fibroblasts of cardiac origin. *Circ Res*. 2003;93:421-428.
15. Rohr S, Kucera JP. Involvement of the calcium inward current in cardiac impulse propagation: Induction of unidirectional conduction block by nifedipine and reversal by bay k 8644. *Biophys J*. 1997;72:754-766.
16. Rohr S, Kucera JP, Fast VG, Kleber AG. Paradoxical improvement of impulse conduction in cardiac tissue by partial cellular uncoupling. *Science*. 1997;275:841-844.
17. Kucera JP, Kleber AG, Rohr S. Slow conduction in cardiac tissue, ii: Effects of branching tissue geometry. *Circ Res*. 1998;83:795-805.
18. Rohr S, Kucera JP, Kleber AG. Slow conduction in cardiac tissue, i: Effects of a reduction of excitability versus a reduction of electrical coupling on microconduction. *Circ Res*. 1998;83:781-794.
19. Miragoli M, Gaudesius G, Rohr S. Electrotonic modulation of cardiac impulse conduction by myofibroblasts. *Circ Res*. 2006;98:801-810.
20. Fast VG, Kleber AG. Microscopic conduction in cultured strands of neonatal rat heart cells measured with voltage-sensitive dyes. *Circ Res*. 1993;73:914-925.
21. Restivo M, Caref EB, Kozhevnikov DO, El-Sherif N. Spatial dispersion of repolarization is a key factor in the arrhythmogenicity of long qt syndrome. *J Cardiovasc Electrophysiol*. 2004;15:323-331.

Supplemental Movie Legends

Movie I: Representative example of simultaneous optical mapping of three host-donor strands which enabled increased experimental throughput.

Movie II: Action potential propagation across host-donor interface of ExF-NRVM and ExS-NRVM strand upon stimulation from either the donor cell end (shown first) or the host NRVM end (shown last) of the strand. Note the slower conduction in the ExS cells and that across all host-donor interfaces, the activation and repolarization wavefronts move in the same direction when the AP travels up the APD gradient (from ExS or ExF to NRVM) but in opposite directions when the AP travels down the APD gradient (from NRVM to ExS or ExF).

Movie III: Effects of $BaCl_2$ application on action potential propagation and repolarization across the ExF-NRVM interface. Note that increased doses of $BaCl_2$ progressively prolonged ExF repolarization and consequently reduced the repolarization gradient across the ExF-NRVM interface.

Movie IV: Effect of $BaCl_2$ application on S2 stimulus block in host-donor strands. An S1-S2 interval of 150 ms or 200 ms leads to S2 block in ExF-NRVM or ExS-NRVM strand, respectively. Note that block occurs beyond heterocellular interface in ExF-NRVM strands and at interface in ExS-NRVM strands. Application of 50 µmol/L $BaCl_2$ to the ExS-NRVM strand restores successful S2 propagation at S1-S2=200 ms.